Effect of femoral mechanical properties on primary stability of cementless total hip arthroplasty: a finite element analysis

Michael Reimeringer[*] and Natalia Nuño[a]

Laboratoire de recherche en imagerie et orthopédie,Département de génie de la production automatisée, École de technologie supérieure 1100 rue Notre-Dame Ouest, Montréal, Québec, H3C 1K3, Canada

Abstract. With the goal of increasing the survivorship of the prosthesis and anticipating primary stability problems of new prosthetic implants, finite element evaluation of the micromotion, at an early stage of the development, is mandatory. This allows assessing and optimizing different designs without manufacturing prostheses. This study aimed at investigating, using finite element analysis (FEA), the difference in the prediction of the primary stability of cementless hip prostheses implanted into a Sawbones® 4th generation, using the manufacturer's mechanical properties and using mechanical properties close to that of human bone provided by the literature (39 papers). FEA was carried out on the composite Sawbones® implanted with a straight taper femoral stem subjected to a loading condition simulating normal walking. Our results show that micromotion increases with a reduction of the bone material properties and decreases with the augmentation of the bone material properties at the stem-bone interface. Indeed, a decrease of the cancellous Young modulus from 155MPa to 50MPa increased the average micromotion from 29 μm up to 41 μm (+42%), whereas an increase of the cancellous Young modulus from 155MPa to 1000MPa decreased the average micromotion from 29 μm to 5 μm (-83%). A decrease of cortical Young modulus from 16.7GPa to 9GPa increase the average global micromotion from 29 μm to 35 μm (+33%), whereas an increase of the cortical Young modulus from 16.7GPa to 21GPa decreased the average global micromotion from 29 μm to 27 μm (-7%). It can also be seen that the material properties of the cancellous structure had a greater influence on the micromotion than the material properties of the cortical structure. The present study shows that micromotion predicted at the stem-bone interface with material properties of the Sawbones® 4th generation is close to that predicted with mechanical properties of human femur.

Keywords: total hip arthroplasty; cementless stem; primary stability; material properties; finite element analysis

1. Introduction

Total hip arthroplasty (THA) consists in removing the head and neck of a femur and replacing them by prosthesis to relieve pain and restore joint function. Although it is a successful intervention, failures have led to search for alternative solutions such as new designs, new materials, new fixation methods, or also new surgical instrumentations, in the hope of increasing

---

*Corresponding author, Ph.D, E-mail: mickareim@gmail.com
[a] Professor, E-mail: Natalia.Nuno@etsmtl.ca

the survivorship of the prosthesis.

There exist two types of prosthetic devices: cemented and cementless stems. Cemented stems are fixed to the surrounding bone by means of bone cement, whereas cementless stems are fixed to the surrounding bone by mechanical press-fit. Debate remains concerning the best fixation method, nevertheless short-, mid-, and long term outcomes are good for both fixations (Pivec *et al.* 2012). However, deterioration of cement over the time introduces wear debris, thus making revision surgery more complicated. Nonetheless, with cementless stem, concerns exist about the risk of failure in terms of primary stability and hence secondary osteointegration. It has been shown that motion at the bone-implant interface around 40 μm produces partial ingrowth, while motion at the bone-implant interface exceeding 150 μm completely inhibits bone ingrowth (Pilliar *et al.* 1986).

Development of new prosthetic devices implies many iterations between computer aided design (CAD), testing and clinical evaluations. Testing of the initial stability of new prosthetic devices can be assessed either by in-vitro or by finite element analysis (FEA) studies. In-vitro studies imply to dispose of prosthesis prototypes, cadaveric or composite bones, gauges and also mechanical devices to evaluate the motion at the bone-implant interfaces. FEA has the advantage to be made at an early stage of the development, before prototypes of prosthesis are made. It also allows evaluation of different designs and optimization of the design with minimal resources compared to experiments. The use of FEA imposes to dispose of various factors such as the geometry of the models, the applied boundary conditions, and the material properties of the different structures involved. These factors are crucial for the reliability of the results (Baca *et al.* 2008). Indeed, (Reimeringer *et al.* 2013a) have shown that primary stability achieved after implantation is directly influenced by the length and design of the stem. (Pancanti *et al.* 2003) also showed that the inter-subject variability and inter-task variability influence the primary stability of cementless implant.

The 3D geometry of the models can be reconstructed from medical images such as computed tomography (CT) scan to create a personalised femur. A composite bone can also be used as proposed by (Viceconti *et al.* 1996). It has the advantage of eliminating geometric variance problems and mechanical variability between cadaveric femurs when performing experiments. The use of composite bone over human specimens has many other advantages: ease of storage, lack of toxicity, reasonable cost, no degradation in quality with time, and low interspecimen variability (Papini *et al.* 2007). The only composite bone commercially available on the market is Sawbones® 4th generation (Pacific Research Laboratory Inc., Vashon Island, WA, USA). Its mechanical behaviour has been validated by (Heiner 2008) and (Gardner *et al.* 2010). The composite Sawbones® is commonly used in in-vitro or FEA pre-clinical studies to investigate different parameters by many investigators (Duda *et al.* 1998, Baleani *et al.* 2000, Viceconti *et al.* 2000, Viceconti *et al.* 2001, Tomsen *et al.* 2002, Cristofolini *et al.* 2003, Kassi *et al.* 2005, McKellop *et al.* 2005, Speirs *et al.* 2007a, Speirs *et al.* 2007b, Grant *et al.* 2007, Park *et al.* 2008, Park *et al.* 2009, and Thielen *et al.* 2009).

The 3D femur geometry of the Sawbones® 4th generation is available on the Biomedical Research Community website (www.biomedtown.org). This composite femur is made of two materials: short fiber filled epoxy for the cortical bone analogue and rigid polyurethane foam for the cancellous bone analogue. The behaviour of each material has been characterized as isotropic homogeneous (Table 1), whereas the behaviour of a human femur is mainly anisotropic heterogeneous (Wirtz *et al.* 2000).

Indeed, mechanical properties of cortical and cancellous human femur have been characterized by investigators in many experimental studies (see Appendix A & B). Parameters such as Young

Table 1 Material properties of the Sawbones® fourth-generation (Sawbones® 2013)

	Density	Longitudinal tensile		Compressive		Transverse tensile	
		Strength	Modulus	Strength	Modulus	Strength	Modulus
	(g/cm^3)	(MPa)	(GPa)	(MPa)	(GPa)	(MPa)	(GPa)
Cortical bone (short fiber filled epoxy)	1.64	106	16	157	16,7	93	10
Cancellous bone (rigid polyurethane foam)	0,27	--	--	6	0,155	--	--

modulus (E), Poisson coefficient (v), yield stress (σ_y) or also ultimate stress (σ_u) have been measured under various testing methods, the most common being axial compression or tension tests. A significant scatter in the material properties are found in the published data. Appendix A and B show that Young modulus of the cortical bone varies from E= 9GPa to 22GPa and the cancellous bone varies from E= 77MPa to 601MPa for the same anatomic site using the same test methods. Many investigators (Wall *et al.* 1979, Keller *et al.* 1990, Goldstein 1987, Majumbar *et al.* 1998, Wirtz *et al.* 2000, Helgasson *et al.* 2008, Jirousek 2012) explain this broad discrepancy by various factors:

- The origin, age, gender of the subject;
- The size, anatomic location, structural architecture, orientation, geometry and physical characteristics of the specimens tested;
- The method of storage, preparation and moisture of the specimens tested;
- The testing method, loading direction and stain rate.

Very few studies aimed at assessing the effect of material properties of the bone on the implant primary stability. (Wong *et al.* 2005) investigated the effect of a uniform reduction of Young's modulus of the femur by 10, 20, 30 and 40 per cent on the implant stability. They also studied the effect of a reduction of the cortical Young modulus by 0 and 20 per cent, both combined with a reduction of cancellous Young modulus by 40 per cent that can simulate bone density changes with ageing. They found that changes to the bone modulus will affect the micromotion at the stem-bone interface. In addition, (Bryan *et al.* 2010) emphasized that primary stability of a hip implant can vary between pre-clinical testing (FEA or in vitro studies) and once implanted in the patient.

Therefore, the aim of this numerical study is to investigate the effect of material properties assignments of the cortical and cancellous bones on the primary stability of a cementless prosthesis into a composite bone. The primary stability is defined by the micromotion predicted at the stem-bone interface of a Sawbones® 4th generation using the manufacturer's given mechanical properties and using mechanical properties closer to that of human bone from 39 articles of the literature.
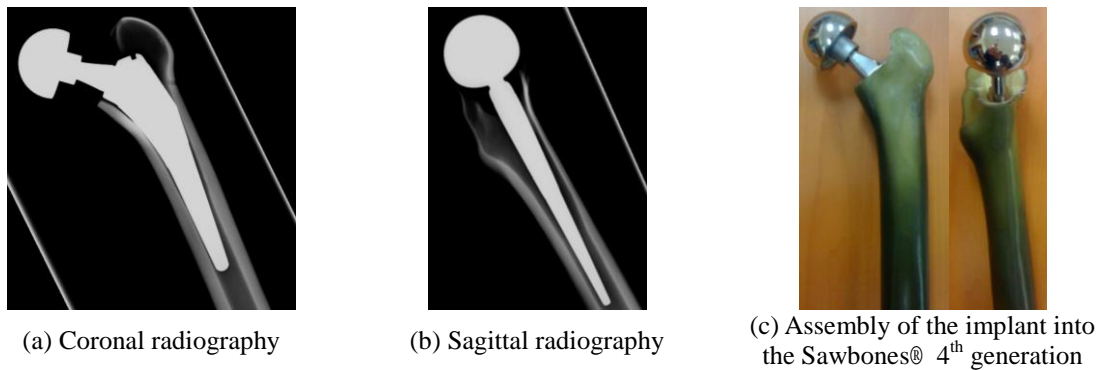
(a) Coronal radiography   (b) Sagittal radiography   (c) Assembly of the implant into the Sawbones® 4th generation

Fig. 1 Experimental implantation

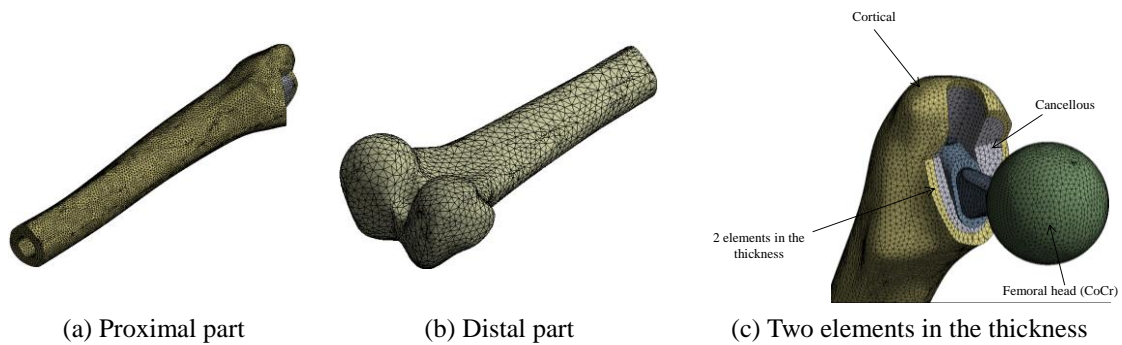(a) Proximal part   (b) Distal part   (c) Two elements in the thickness

Fig. 2 Illustration of the mesh construct

2. Materials and Methods

A virtual implantation of a straight Profemur® TL (Wright Medical Technology Inc., Arlington, TN, USA) was performed into a Sawbones® 4th generation (Mod. 3406) using CatiaV5R19 (Dassault Systèmes, Velizy Villacoublay, France). A size 6 Profemur® TL stem, corresponding to the middle of the stem range sizes, was chosen based on an experimental implantation (Fig. 1). The implant position and orientation was validated in a previous study (Reimeringer *et al.* 2013a).

The 3D model was transferred into Ansys Workbench 13.0 (Ansys Inc., Canonsburg, PA, USA) pre- and post- processing program. A tetrahedral (10 nodes) mesh was created. (Helgasson, *et al.* 2008) studied the sensitivity of the mesh size. They showed that an average mesh size of 3.3mm is a threshold to obtain satisfactory convergence. Moreover, (Reimeringer *et al.* 2008) recommended a minimum of two elements in the thickness of the structure. Thus, a mesh size of 2mm was generated proximally (Fig. 2(a)), whereas a mesh size of 5mm (Fig. 2(b)) was generated distally, as this region was away from the region of interest. Fig. 2(c) shows the two elements in the thickness of the cortical structure.

FEA was carried out for the static loading conditions defined by (Bergmann *et al.* 2001), simulating normal walking being the most common physiological activity (Morlock *et al.* 2001). The applied resultant forces (calculated with a body weight of 836N) were 871N and 1948N to simulate the abductor muscles and hip joint contact forces, respectively (Fig. 3(a)). The femoral condyles were assumed to be rigidly constrained in all directions (Fig. 3(b)). The resultant forces

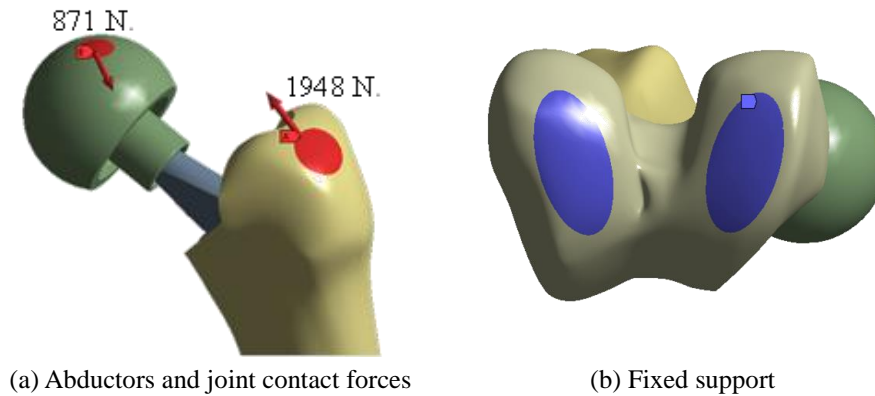(a) Abductors and joint contact forces   (b) Fixed support

Fig. 3 Boundary conditions

were oriented in the coordinate system defined by (Bergmann *et al.* 2001) where z-axis is parallel to the idealised midline of the femur and the x-axis is parallel to the dorsal contour of the femoral condyles in the transverse plane.

Contacts between bone and the prosthesis were assumed all along the prosthesis with the exception of an area above the plasma spray. The stem-bone contact interface was modelled using the augmented Lagrange algorithm with face to face contact element (Viceconti *et al.* 2000), with the prosthesis as the contact body and the femoral cavity as the target body. To represent more realistically the contact between the stem and the bone, the stem-bone contact interface was divided into four zones (Fig. 4) based on (Reimeringer *et al.* 2013a): the plasma spray surface in contact with cortical bone defined as frictional with a press-fit (Fig. 4(a)); the plasma spray superior surface in contact with cancellous bone, defined as frictional without press-fit (Fig. 4(b)); the plasma spray inferior surface in contact with cancellous bone defined as frictional with a press-fit (Fig. 4(c)); the polished inferior surface of the stem in contact with cancellous bone defined as frictional without press-fit (Fig. 4(d)) and finally a part of the polished superior surface of the stem located above the plasma spray in contact with cancellous bone, defined as frictional without press-fit (Fig. 4(e)). The press-fit was simulated with an interference of 0.05mm (Abdul Kadir *et al.* 2008). The frictional contact μ was set to 0.6 for the plasma spray surface and 0.08 for the polished surface (Grant *et al.* 2007). The convergence was checked for force and displacement with a tolerance of 1%.

The stem was made of titanium with a Young modulus (E) set at 110GPa, whereas the head was made of chrome-cobalt, with E set at 210GPa. Material properties of the composite Sawbones® 4th generation (Table 1) defined as isotropic homogeneous were used as reference (Table 2, Analyses 1). To further understand the influence of material properties of the human femur on the primary stability, 11 finite element analyses (FEA) were performed with different assignments of material properties for the cortical and cancellous composite Sawbones® 4th generation (Table 2).

First, the cortical Young modulus E was defined as isotropic homogeneous and set at 16.7GPa with a variation of the cancellous Young modulus (Table 2, Analyses 2), also defined as isotropic homogeneous with values set as follow: 50MPa, a value close to that found by (Majumbar *et al.* 1998), 100MPa, an intermediate value, 300MPa, a value close to that found by (Brown *et al.* 1980), 500MPa, a value close to that found by (Morgan *et al.* 2001a) and 1000MPa, an extreme value

Table 1 Values of cancellous and cortical Young modulus E used in the finite element analysis

	Young modulus E of cancellous bone (MPa)	Young modulus E of cortical bone (GPa)	Analyses
Reference	155	16.7	1
Isotropic cancellous variation	50	16.7	2
	100		
	300		
	500		
	1000		
Orthotropic cancellous variation	Superior-inferior = 133 Medial-lateral = 62 Anterior-posterior = 53	16.7	3
Isotropic cortical variation	155	9	4
		12.5	
		18.5	
		21	

(a) Plasma spray surface with the cortical bone

(b) Plasma spray superior surface with cancellous bone

(c) Plasma spray inferior surface with cancellous bone

(d) Polished inferior surface with cancellous bone

(e) Polished superior surface with cancellous bone
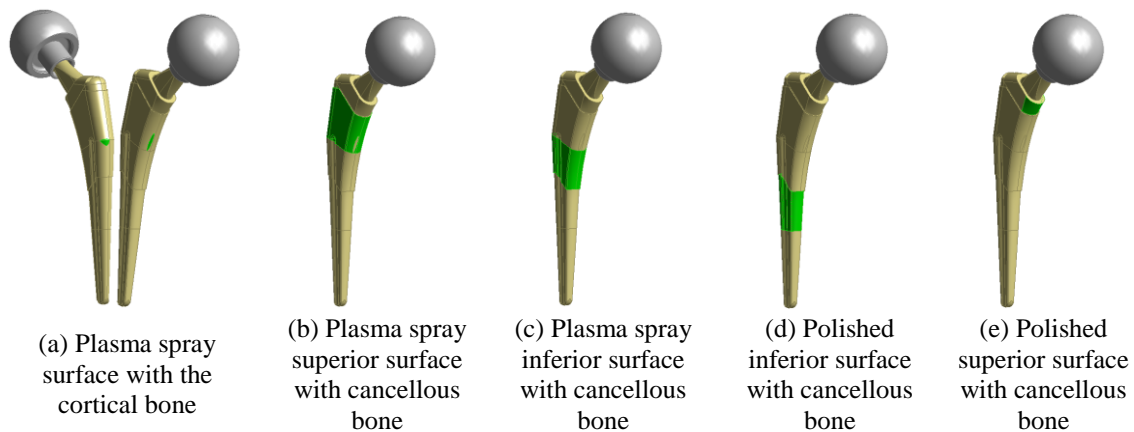
Fig. 2 Stem-bone contact interface

value chosen to see whether a trend in the results could be observed. These values of cancellous Young modulus come from literature compression tests realised with samples extracted in the proximal part or the great trochanter of the femur (Appendix A). We have excluded values provided from samples located in the head and the neck due to the fact that these regions are removed during THA surgery. Then, the material properties of the cancellous bone were defined as orthotropic homogeneous with a Young modulus E set at 133MPa, 62MPa and 53MPa for the superior-inferior (SI), medial-lateral (ML) and antero-posterior (AP) directions, respectively (Table 2, Analyses 3). These values represent the mean Young modulus found by (Augat *et al.*

(a) Anterior surface   (b) Posterior surface   (c) Lateral surface   (d) Medial surface

Fig. 3 Points where the micromotion is extracted
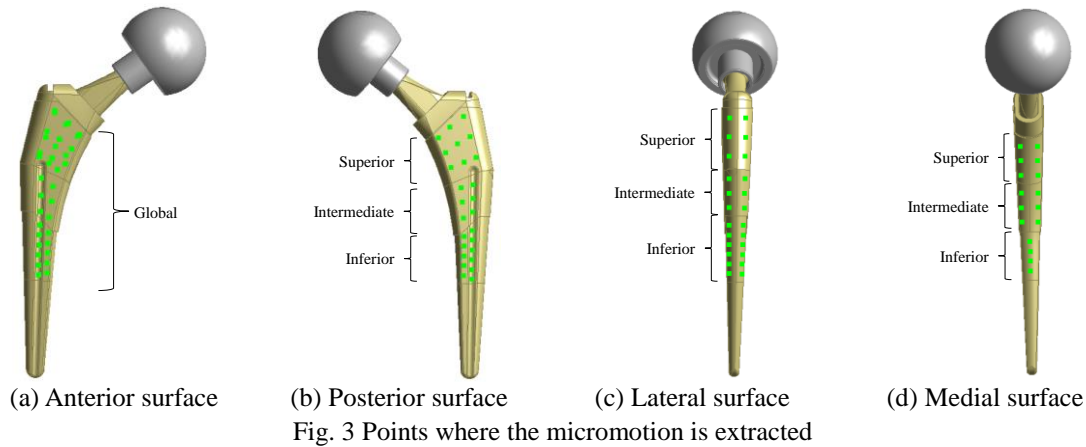
1998) and (Majumbar *et al.* 1998) in the proximal femur (from Appendix A). Afterward, FEA were performed with the cancellous Young modulus, defined as isotropic homogeneous, set at 155MPa with a variation of the cortical Young modulus (from Appendix B), also defined as isotropic homogeneous, with values set as follow: 9GPa, 12.5GPa, 18.5GPa and 21GPa (Table 2, Analyses 4). The Poisson ratio for all materials in all configurations was set to 0.3.

Since the measurement of micromotion at one single point is not sufficient to describe the stability of a femoral stem (Ostbyhaug *et al.* 2010), the micromotion (μm) was extracted on 92 points distributed all along the stem (Fig. 5) by calculating the difference between the final displacement of the prosthesis and the final displacement of the bone. Fifty two (52) points were located on the anterior (Fig. 5(a)) and posterior (Fig. 5(b)) surfaces (twenty six (26) on each face): of which thirty (30) on the plasma spray surface and twenty two (22) on the polished surface. Twenty four (24) points were located on the lateral surface (Fig. 5(c)): of which twelve (12) on the plasma spray surface and twelve (12) on the polished surface. Sixteen points (16) were located on the medial surface (Fig. 5(d)): of which twelve (12) on the plasma spray surface and four (4) on the polished surface.

The results of the average micromotion will be presented on several divisions of the implant (Fig. 5): the superior area, plasma spray area where no press-fit is applied, which represents 30 points; the intermediate area, plasma-spray surface where press-fit is applied, which represents 24 points, the inferior area, polished surface without press-fit, which represents 38 points and the global area, which represents all 92 points. Afterward, average micromotion will be presented on each of the four faces; the posterior and inferior faces, which represent 26 points on each face; the medial face, which represents 16 points and the lateral face, which represents 24 points. The Von Mises distribution within the cancellous and cortical bones located at three different locations of the stem will also be presented.

3. Results

Table 3 and Fig. 6 show the average value of micromotion, corresponding standard deviation and the range at the stem-bone interface with variations of the cancellous Young modulus (for cortical Young modulus constant at E=16.7GPa) for the global, superior, intermediate and inferior

Table 2 Average values and standard deviations (±SD) and range of micromotions (μm) with variation of cancellous Young modulus E and cortical Young modulus E=16.7GPa for global (considering 92 points) and for superior, intermediate and inferior parts of the stem

| Young modulus E	Global ±SD(μm)	Range (μm)	Superior ±SD(μm)	Range (μm)	Intermediate ±SD(μm)	Range (μm)	Inferior ±SD(μm)	Range (μm)
Cancellous 50MPa	41±31	0-120	24±21	0-82	25±19	4-50	64±29	21-120
Cancellous 100MPa	32±23	0-87	20±18	0-78	25±19	4-51	47±21	16-87
*Cancellous 155MPa**	*29±19*	*0-78*	*19±17*	*0-78*	*24±18*	*5-51*	*39±17*	*15-71*
Cancellous 300MPa	25±16	0-79	18±17	0-79	25±19	3-53	30±12	13-52
Cancellous 500MPa	23±15	1-79	19±17	1-79	25±19	5-54	25±9	12-42
Cancellous 1000MPa	5±8	0-48	3±9	0-48	10±8	2-25	4±5	0-11
Cancellous orthotropic	35±16	6-100	21±19	0-78	25±19	3-51	52±23	24-100

*Cancellous 155MPa: Sawbones® properties
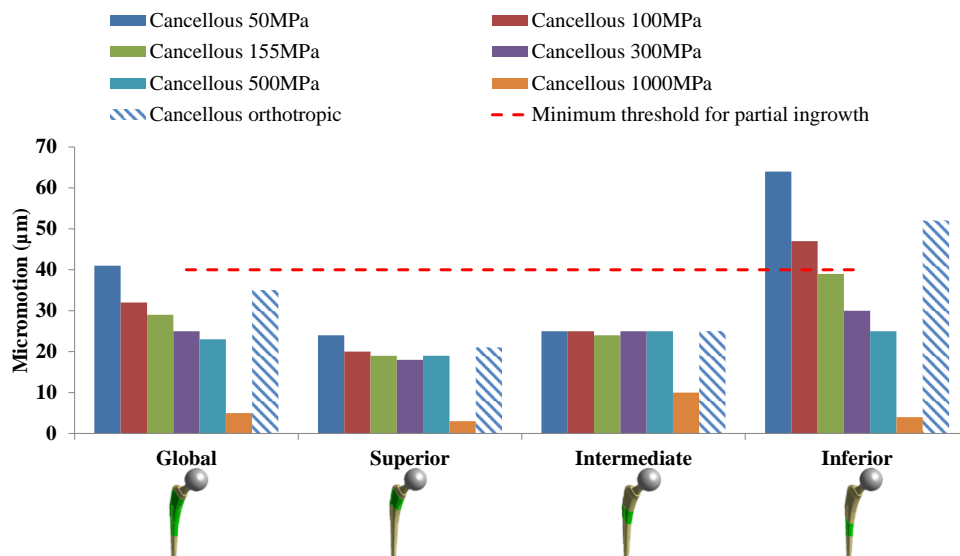
Fig. 4 Average global, superior, intermediate and inferior micromotions (μm) with variation of cancellous Young modulus E and cortical Young modulus E = 16.7GPa

part of the prosthesis for normal walking loading conditions. A decrease of the cancellous Young modulus from E=155MPa (Young modulus of the composite Sawbones® 4th generation) to 50MPa increased the average global micromotion from 29 μm up to 41 μm (+42%), the average superior micromotion from 19μm up to 24 μm (+26%), the average intermediate micromotion from 24 μm to 25 μm (+4%) and the average inferior micromotion from 39 μm up to 64 μm (+64%). However, an increase of the cancellous Young modulus from E=155MPa to 1000MPa decreased the average global micromotion from 29 μm to 5 μm (-83%), the average superior micromotion from 19 μm to 3 μm (-84%), the average intermediate micromotion from 24 μm to 10 μm (-58%) and the average inferior micromotion from 39 μm to 4 μm (-90%).

When cancellous Young modulus is defined as orthotropic (E_{SI} = 133MPa; E_{ML} = 62MPa; E_{AP} = 53MPa), compared to that of composite Sawbones® 4th generation (E = 155MPa) the average global micromotion increased up to 35 μm (+21%), up to 21 μm (+11%) for the average superior micromotion, up to 25 μm (+4%) for the average intermediate micromotion and up to 52 μm (+33%) for the average inferior micromotion, as shown in Table 3 and Fig. 6.

Table 4 and Fig. 7 show the average value of micromotion, corresponding standard deviation at the stem-bone interface with variations of the cancellous Young modulus (for cortical Young modulus constant E=16.7GPa) for the posterior, anterior, medial and lateral faces of the stem. A decrease in the cancellous Young modulus from E = 155MPa (Young modulus of the composite Sawbones® 4th generation) to 50MPa increased the average posterior micromotion from 21 μm up to 34 μm (+62%), the average anterior micromotion from 27 μm up to 40 μm (+48%), the average medial micromotion from 38 μm up to 50 μm (+32%) and the average lateral micromotion from 32 μm up to 41 μm (+28%). However, an increase in the cancellous Young modulus from E=155MPa to 1000MPa decreased the average posterior micromotion from 21μm to 2μm (-90%), the average anterior micromotion from 27 μm to 8 μm (-70%), the average medial micromotion from 38μm to 9 μm (-76%) and the average lateral micromotion from 32 μm to 5 μm (-84%).

When cancellous Young modulus is defined as orthotropic (E_{SI} = 133MPa; E_{ML} = 62MPa; E_{AP} = 53MPa), compared to that of composite Sawbones® 4th generation (E = 155MPa), the average posterior micromotion increased up to 28 μm (+33%), the average anterior micromotion up to 36 μm (+33%), the average medial micromotion up to 42 μm (+11%) and the average lateral micromotion up to 36 μm (+13%), as shown in Table 4 and Fig. 7.

Table 5 and Fig. 8 show the average value of micromotion, corresponding standard deviation and the range at the stem-bone interface with variations of the cortical Young modulus (for cancellous Young modulus constant at E=155MPa) for the global, superior, intermediate and inferior parts of the stem. A decrease in the cortical Young modulus from E=16.7GPa (Young modulus of the composite Sawbones® 4th generation) to 9GPa increased the average global micromotion from 29 μm to 35 μm (+21%), the average superior micromotion from 19 μm to 20 μm (+5%), the average intermediate micromotion from 24 μm to 25 μm (+4%) and the average inferior micromotion from 39 μm to 52 μm (+33%). However, an increase of the cortical Young modulus from E=16.7GPa to 21GPa decreased the average global micromotion from 29 μm to 27 μm (-7%) and the average inferior micromotion from 39 μm to 34 μm (-13%), whereas the average superior and intermediate micromotions did not change.

Table 6 and Fig. 9 show the average value of micromotion, corresponding standard deviation at the stem-bone interface with variations of the cortical Young modulus (for cancellous Young modulus constant at E=155MPa) for the posterior, anterior, medial and lateral faces of the stem. A decrease in the cortical Young modulus from 16.7GPa (Young modulus of the composite Sawbones® 4th generation) to 9GPa increased the average posterior micromotion from 21 μm to

Table 3 Average values and standard deviation (±SD) of micromotions (μm) with variation of cancellous Young modulus E and cortical Young modulus E=16.7GPa for posterior, anterior, medial and lateral faces of the stem

Young modulus E	Posterior ±SD (μm)	Anterior ±SD (μm)	Medial ±SD (μm)	Lateral ±SD (μm)
Cancellous 50MPa	34±40	40±32	50±28	41±17
Cancellous 100MPa	25±28	31±25	42±20	35±13
Cancellous 155MPa	***21±22***	***27±21***	***38±16***	***32±11***
Cancellous 300MPa	17±15	23±18	34±14	29±10
Cancellous 500MPa	15±11	22±16	32±13	29±11
Cancellous 1000MPa	2±1	8±10	9±10	5±7
Cancellous orthotropic	28±31	36±29	42±22	36±14

*Cancellous 155MPa: Sawbones® properties
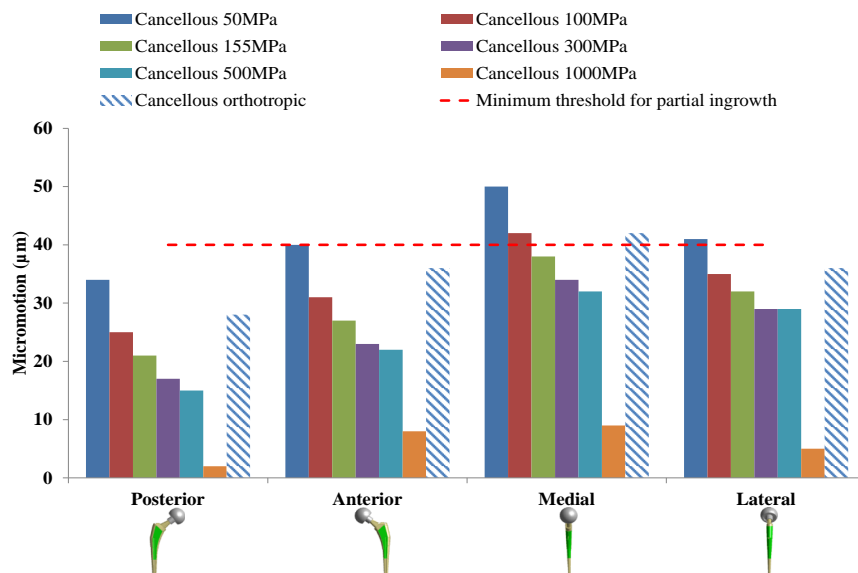
Fig. 5 Average posterior, anterior, medial and lateral micromotions (μm) with variation of cancellous Young modulus E and cortical Young modulus E=16.7GPa

Table 4 Average values and standard deviation (±SD) and range of micromotions (µm) with variation of cortical Young modulus E and cancellous Young modulus E=155MPa for global (considering 92 points) and for superior, intermediate, inferior parts of the stem

Young modulus E	Global ±SD(µm)	Range (µm)	Superior ±SD(µm)	Range (µm)	Intermediate ±SD(µm)	Range (µm)	Inferior ±SD(µm)	Range (µm)
Cortical 9GPa	35±27	0-117	20±23	0-117	25±19	6-55	52±26	13-105
Cortical 12.5GPa	31±22	0-93	20±19	0-93	26±18	5-52	44±21	14-84
*Cortical 16.7GPa**	*29±19*	*0-78*	*19±17*	*0-78*	*24±18*	*5-51*	*39±17*	*15-71*
Cortical 18.5GPa	28±18	0-71	19±17	0-71	26±19	5-55	36±15	16-65
Cortical 21GPa	27±17	0-65	19±17	0-65	24±19	4-50	34±13	16-59

*Cortical 16.7GPa: Sawbones® properties
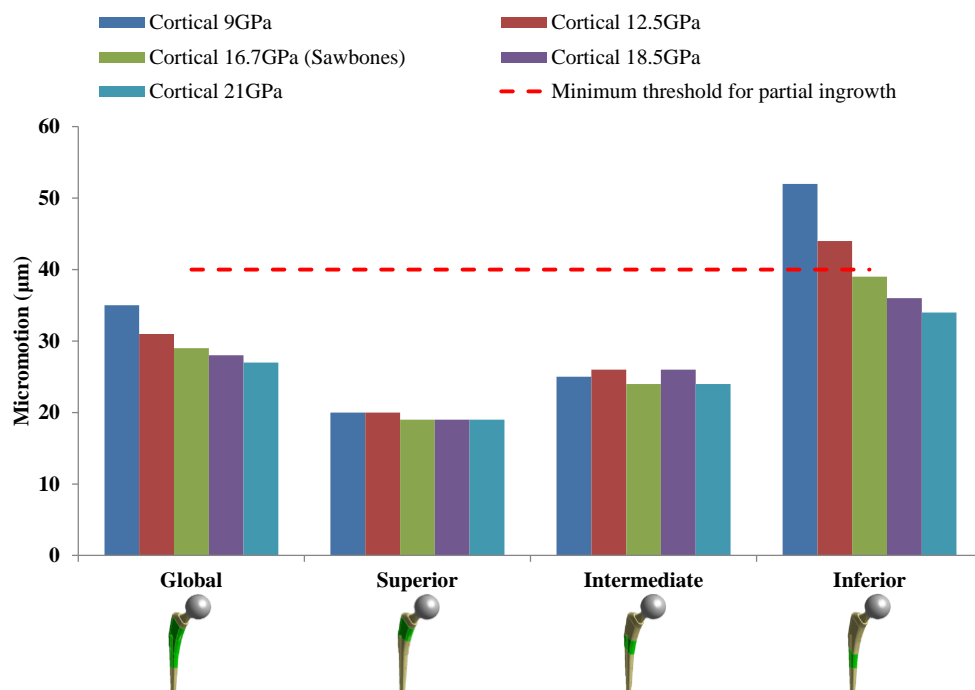
Fig. 6 Average global, superior, intermediate and inferior micromotions (µm) with variation of cortical Young modulus E and cancellous Young modulus E=155MPa

Table 5 Average value and standard deviation (±SD) of micromotion (μm) with variation of cortical Young modulus E and cancellous Young modulus E=155MPa for posterior, anterior, medial and lateral faces of the stem

Young modulus E	Posterior ±SD(μm)	Anterior ±SD(μm)	Medial ±SD(μm)	Lateral ±SD(μm)
Cortical 9GPa	27±32	34±31	45±24	38±15
Cortical 12.5GPa	25±27	30±25	40±19	34±12
*Cortical 16.7GPa**	*21±22*	*27±21*	*38±16*	*32±11*
Cortical 18.5GPa	22±21	26±20	37±15	32±11
Cortical 21GPa	19±19	25±18	36±14	31±11

Cortical 16.7GPa: Sawbones® properties

Fig. 7 Average posterior, anterior, medial and lateral micromotions (μm) with variation of cortical Young modulus E and cancellous Young modulus E=155MPa

27 μm (+29%), the average anterior micromotion from 27 μm to 34 μm (+26%), the average medial micromotion from 38 μm to 45 μm (+18%) and the average lateral micromotion from 32 μm to 38 μm (+19%). However, an increase in the cortical Young modulus from E=16.7GPa to 21GPa slightly decreased the average posterior micromotion from 21 μm to 19 μm (-10%), the average anterior micromotion fr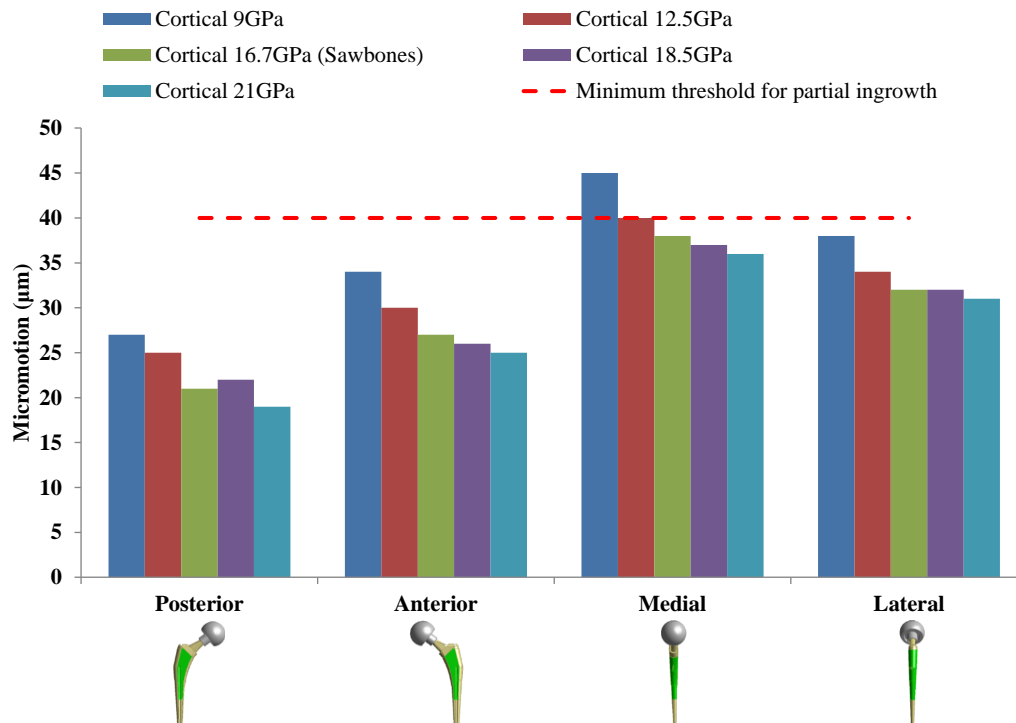om 27 μm to 25 μm (-7%), the average medial micromotion from 38 μm to 36 μm (-5%) and the average lateral micromotion from 32 μm to 31 μm (-3%).

Fig. 10 shows the Von Mises stress distribution within the implanted Sawbones® as a function of cancellous Young modulus, with cortical Young modulus E=16.7GPa. In the superior part, for a variation of the cancellous Young modulus from 50MPa to 500MPa, Von Mises stress distribution is very similar. The stress remains under 1MPa in the cancellous bone and lower than 20MPa in the cortical bone, with a maximum reached in the anterior side. When the cancellous Young modulus increases up to 1000MPa, Von Mises stress increases in the cancellous structure up to 4MPa. In the cortical structure, Von Mises stress is more homogeneous, being lowest in the posterior direction. In the intermediate part, Von Mises stress distribution increases with the increase of the cancellous Young modulus. In the cancellous structure, Von Mises stress distribution increases mainly in the medial and lateral directions, followed by the anterior and posterior directions. In the cortical structure, Von Mises stress increases mainly in the medial, lateral and anterior direction, always remaining lower than 39MPa, with a maximum reached in the medial direction of the cortical structure. In the inferior part, an increase of the cancellous Young modulus up to 500MPa increases the Von Mises stress in the lateral direction of cancellous structure. An increase of the cancellous Young modulus E up to 1000MPa increases mainly the Von Mises stress distribution within the cancellous structure. In the cortical structure, the Von Mises stress is higher in the lateral and medial directions.

Fig. 11 shows the Von Mises stress distribution within the implanted Sawbones® as a function of the cortical Young modulus, with cancellous Young modulus E=155MPa. In the superior part, an increase of the cortical Young modulus mainly increases the Von Mises stress within the medial and anterior directions of the cortical structure. The maximum is always reached on the anterior side. Von Mises stress within the cancellous structure remains lower than 1MPa. In the intermediate part, maximum Von Mises stress is located in the medial and anterior directions of the cortical structure. In the cancellous structure, Von Mises stress is lower than 2MPa with the exception of the medial and lateral direction where the Von Mises stress increases up to 4MPa. In the inferior part, Von Mises stress in the cancellous structure is lower than 1MPa, with the exception of the lateral directions where the Von Mises stress increases up to 3MPa. In the cortical structure, Von Mises stress is higher in the lateral and medial directions than in the anterior and posterior directions. Maximum is reached in the lateral direction of the cortical structure.

4. Discussion

Many uncemented femoral stem designs have shown excellent long-term survivorship (Garelick *et al.* 2009). With the goal of improving the life of the prosthesis and anticipating primary stability problems of new prosthetic components, finite element evaluation of the micromotion, at an early stage of the development, is mandatory. This allows assessing and optimizing different designs without manufacturing prostheses. This study aimed at investigating, using FEA, the difference in the prediction of the primary stability of cementless hip prostheses implanted into a Sawbones® 4th generation, using the manufacturer's mechanical properties and using mechanical properties

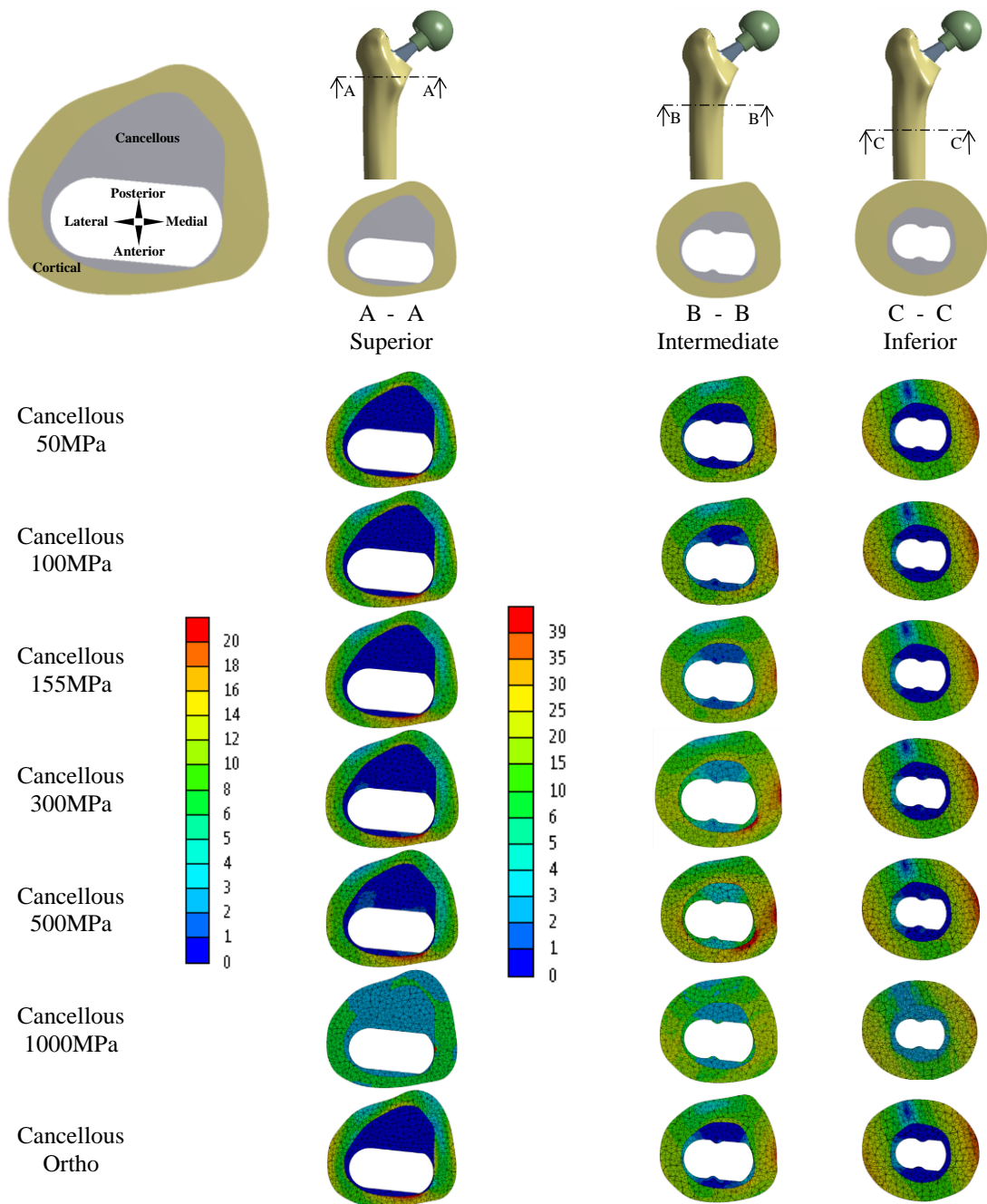close to that of human bone provided by almost 40 articles from the literature.

Fig. 8 Von Mises stress (MPa) within the implanted Sawbones® with variation of cancellous Young modulus and cortical Young modulus E=16.7GPa

Our results show that the global average micromotion, considering all 92 points of the prosthesis, predicted by the mechanical properties of the composite Sawbones® 4th generation and mechanical properties close to that of human bone are similar except for the cancellous Young modulus set to 1000MPa. However, this extreme value was exceptionally not taken from the literature but was chosen to have an indication of the trend. In general, a reduction of either the cortical or cancellous Young modulus leads to an increase of the predicted micromotion at the stem-bone interface. This reduction of Young modulus simulates lesser bone quality. Thus, there is less constraint between the stem and the surrounding bone: the stem can move more easily with respect to the surrounding bone, consequently more micromotion is predicted. Conversely, an increase of the cancellous or cortical Young modulus leads to a decrease of the predicted micromotion. This simulates augmentation of bone quality. Nevertheless, for all variations of either cancellous or cortical Young modulus, the bone-implant interface micromotion predicted in this study remains lower than 150 μm on all 92 points located on the prosthesis. Furthermore, most of the predicted average micromotion remains below 40 μm. These values represent the threshold value with regards to osteointegration (Pilliar *et al.* 1986).

When not considering the global micromotion, the micromotions predicted at plasma spray surface (superior and intermediate parts) and the polished surface (inferior part) of the stem are different. The polished surface is strongly affected by the mechanical properties variations. This phenomenon can be explained by the difference in the friction properties between these two areas. Indeed, for the polished surface of the stem, the friction coefficient (μ=0.08) is lower than that of the plasma-spray surface (μ=0.6). There is also a press-fit of 0.05mm applied on a part of the plasma-spray surface in the intermediate part. This can explain that higher micromotion was found in the inferior part of the stem (polished surface). It can also be seen that for this particular stem design (straight taper femoral stem), micromotion is greater on the anterior and medial faces than on the posterior and lateral faces. Maximums are located on the anterior superior face with the exception of the low cancellous Young modulus assignment of 50MPa and 100MPa, where the maximum local is located on the posterior inferior face.

The results of the present study are partly in accordance with the numerical study of (Wong *et al.* 2005). Indeed, in their study of the anatomic IPS™ stem (DePuy Orthopaedics, Inc, Warsaw, IN, USA) subjected to the static loading condition simulating walking, they also found that the reduction of either the cortical or cancellous bone Young modulus or both increases the stem micromotion. Their range of micromotion was comprised between 10 μm and 90 μm, with maximum located on the lateral face. In general they have found that the cancellous Young modulus had a greater effect on proximal micromotion and the cortical Young modulus on the distal micromotion. Whereas in the present study, Young modulus of cancellous structure had a greater influence than the cortical Young modulus on the micromotion. This difference can be explained by several factors. In the study of (Wong *et al.* 2005), a personalized femur was developed with Young modulus of cancellous and cortical bones defined from the relationship using average apparent density from CT scans. The IPS™ stem design is an anatomical design somewhat different of a straight taper design. They used a higher frictional contact μ for the smooth surface (μ=0.4) and no press-fit was simulated in their study. Their results are also only extracted on the porous coated region of the IPS™ stem. In the present study, a composite femur was used with homogeneous Young modulus and a press-fit in the intermediate part was applied. (Reimeringer *et al.* 2013b) showed that press-fit increases the primary stability. To the author's knowledge, no other study has been carried out so far addressing the influence of the femoral mechanical properties on the primary stability of a cementless stem.
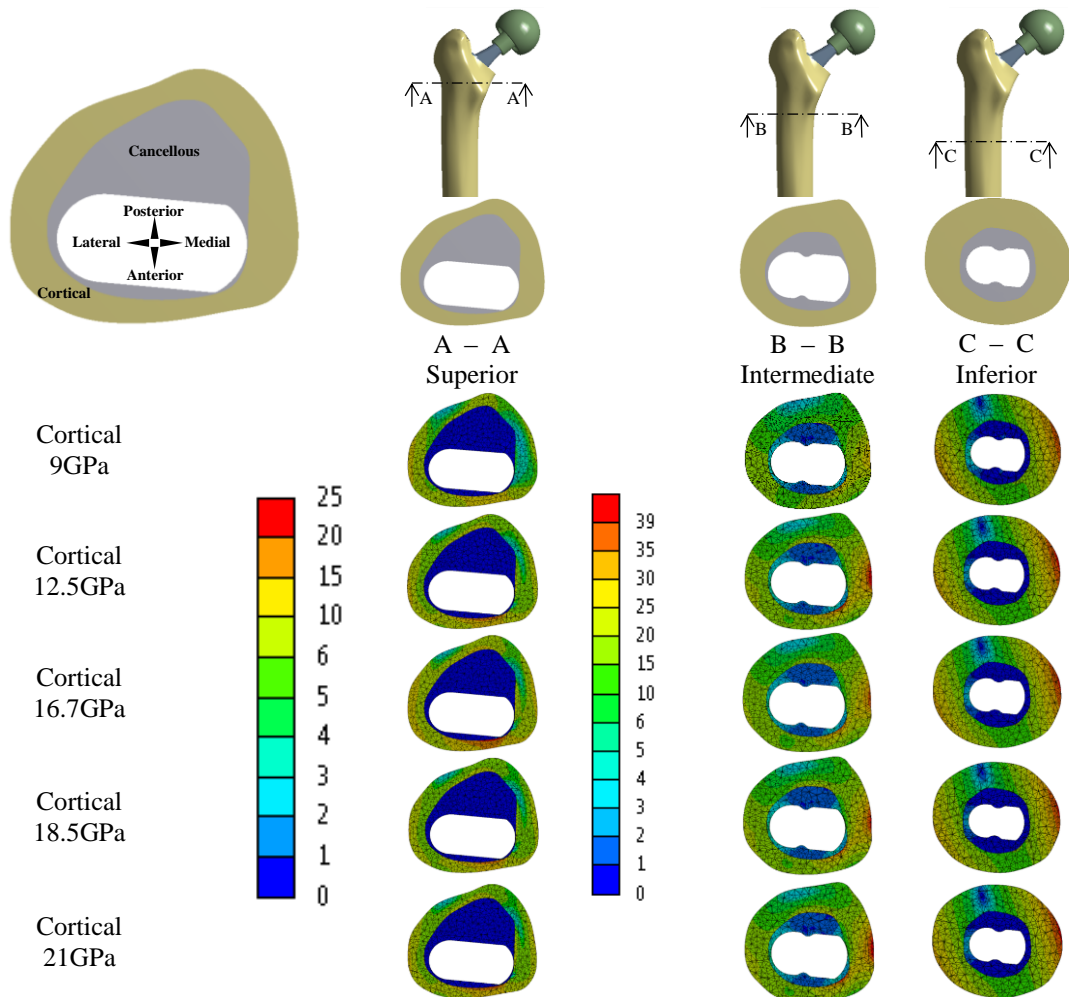
Fig 9 Von Mises stress (MPa) within the implanted Sawbones® with variation of cortical Young modulus and cancellous Young modulus E=155MPa

The predicted micromotion using the cancellous orthotropic properties assignment is higher than that predicted by the composite Sawbones® 4th generation. Although the superior-inferior direction (longitudinal) cancellous Young modulus (133MPa) is close to that of composite Sawbones® 4th generation (155MPa), whereas the medial-lateral (62MPa) and antero-posterior (53MPa) Young modulus is about 3 times lower than that of the composite Sawbones® 4th generation. This can explain the difference in the micromotion results as Young modulus is lower (in 2 of the 3 directions) consequently the micromotion is higher as was explained earlier in the discussion on the overall micromotion.

The results of the Von Mises stress distribution show that variation of cancellous or cortical Young modulus E does not influence the Von Mises stress within the cancellous or cortical structure in the superior and inferior parts with the exception of the cancellous Young modulus E=1000MPa (the extreme value not taken from the literature). However, variation of the

cancellous and cortical Young modulus E increases the Von Mises stress distribution within the cancellous and cortical structures of the intermediate part. Indeed, the Von Mises stress increases when cancellous and cortical Young modulus E increase. This indicates that the load transfer takes place mainly in the intermediate part for this particular stem design, the part of the stem where press-fit is applied. The maximum Von Mises stresses are always located within the cortical structure, in the anterior side for the superior part and in the medial side for the intermediate and inferior parts.

This study presents some limitations. Although material properties of human bone is anisotropic inhomogeneous (Wirtz *et al.* 2000), the material properties used to characterize the composite bone have been defined as isotropic homogeneous, with the exception of one numerical analysis (Table 2, Analyses 3). Peng *et al.* (2006) and Baca *et al.* (2008) found that homogeneous assignment of material properties underestimated global displacement of the femur. (Baca *et al.* 2008) underlined that orthotropic assignment should be used for finite element analysis of very small specimens ($1mm^3$). In their study, they compared the assignment of isotropic and orthotropic inhomogeneous materials on global and small specimens. They obtained a difference of only 4.8% in magnitude displacement for the global specimen, whereas for the small specimen, the difference in magnitude displacement is higher. As in the present study a global micromotion was investigated, small difference can be expected from the fact of assuming isotropic homogeneous material properties instead of orthotropic inhomogeneous.

Another limitation is that in our study, contact between the bone and the prosthesis was assumed all along the plasma spray and a part of the polished surface of the stem. However, (Howard *et al.* 2004) found that only 43% of the stem-bone interface was really in contact in their study on twelve cadaveric femurs, whereas (Wu *et al.* 2004) found 60% of the stem-bone interface was in contact on five cadaveric femurs and more than one third of the implant surface coated with hydroxyapatite had no contact with the bone. (Park *et al.* 2008) underlined that gaps, located in the proximal region, have a pronounced effect on the primary stability of a THA stem. Lesser physical contact between the bone and prosthesis increases the possibility of the prosthesis to subside further inside the femur. This indicates that micromotion found in the present study can be underestimated compared to reality as full contact between stem and bone was simulated. Nevertheless, our study is relevant for comparing the different numerical solutions of the cancellous and cortical material properties assignments for this particular stem design. Moreover, the range of micromotion predicted in this study is comparable to those found in other in-vitro studies that evaluate micromotion of cementless stem implanted into a Sawbones® subjected to physiological loading simulating walking (McKellop *et al.* 2005, Kassi *et al.* 2005, and Park *et al.* 2008). The range of micromotion is also in accordance with other FE studies (Pancanti *et al.* 2003, Abdul Kadir *et al.* 2007, and Reimeringer *et al.* 2013a).

To conclude, the present study shows that micromotion predicted at the stem-bone interface with material properties of the Sawbones® 4th generation is close to that predicted with a wide range of mechanical properties of human femur found in the literature. A reduction of either the cancellous or cortical Young modulus leads to an increase of the predicted micromotion at the stem-bone interface, but lower than the critical value of 150 μm that is known to inhibit the primary stability. Conversely, an increase of the cancellous or cortical modulus leads to a decrease of the predicted micromotion. Thus, Sawbones® 4th generation using the manufacturer's material properties can be used to anticipate primary stability problems of new prosthetic implants at an early stage of the development.

Acknowledgments

References

Abdul Kadir M.R., and Hansen U.N., (2007), "The effect of physiological load configuration on interface micromotion in cementless femoral stems", *Jurnal Mekanical*, **23**, 50-61

Abdul Kadir, M.R., Hansen, U.N., Hansen, U., Klabunde, R., Lucas, D. and Amis, A., (2008), "Finite element modeling of primary hip step stability: the effect of interference fit", *J. Biomech.*, **41**(3), 587-594.

Augat, P., Link, T., Lang, T.F., Lin, J.C., Majumbar, S. and Genant, H.K., (1998), "Anisotropy of the elastic modulus of trabecular bone specimens from different anatomic locations", *Med. Eng. Phys.*, **20**(2), 124-131.

Baca, V., Horak, Z., Mikulenka, P. and Dzupa, V., (2008), "Comparison of an inhomogeneous orthotropic and isotropic materials models used for FE analyses", *Med. Eng. Phys.*, **30**(7), 924-930.

Baleani, M., Cristofolini, L. and Toni, A., (2000), "Initial stability of new hybrid fixation hip stem: Experimental measurement of implant-bone micromotion under torsional load in comparison with cemented and cementless stems", *J. Biomed. Mater. Res.*, **50**(4), 605-615.

Bergmann, G., Deuretzbacher, G., Heller, M., Graichen, F., Rohlmann, A., Strauss, J. and Duda, G.N., (2001), "Hip contact forces and gait patterns from routine activities", *J. Biomech.*, **34**(7), 859-871.

Birnbaum, K., Sindelar, R., Gärtner, J.R., and Wirtz, D.C., (2002), "Material properties of trabecular bone structures", *Surg. Radiol. Anat.*, **23**(6), 399-407.

Brown, S.J., Pollintine, P., Powell, D.E., Davie, M.W.J. and Sharp, C.A., (2002), "Regional differences in mechanical and material properties of femoral head cancellous bone in health and osteoarthritis", *Calcified Tissue Int.*, **71**(3), 227-234.

Brown, T.D. and Ferguson Jr., A.B., (1980), "Mechanical property distributions in the cancellous bone of the human proximal femur", *Acta Orthop. Scand.*, **51**(3), 429-437.

Brown, T.D. and Fergusson, A.B., (1978), "The developmnent of a computational stress analysis of the femoral head", *J. Bone Joint Surg.*, **60**(5), 619-629.

Bryan, R., Mohan, P.S., Hopkins, A., Galloway, F., Taylor, M. and Nair, P.B. (2010), "Statistical modelling of the whole human femur incorporating geometric and material properties", *Med. Eng. Phys.*, **32**, 57-65.

Burgers, T.A., Mason, J., Niebur, G. and Ploeg, H.L., (2008), "Compressive properties of trabecular bone in the distal femur", *J. Biomech.*, **41**(1), 1077-1085.

Burnstein, A.H., Reilly, D.T. and Martens, M., (1976), "Aging of bone tissue: Mechanical properties", *J. Bone Joint Surg.*, **58**(1), 82-86.

Carter, D.R., Caler, W.E., Spengler, D.M. and Frankel, V.H., (1981), "Fatigue behavior of adult cortical bone: The influence of mean strain and strain range", *Acta. Orthop. Scand.*, **52**(2), 481-490.

Courtney, A.C., Hayes, W.C. and Gibson, L.J., (1996), "Age-related differences in post-yield damage in human cortical bone. Experiment and model", *J. Biomech.*, **29**(11), 1463-1471.

Cristofolini, L., Teutonico, A.S., Monti, L., Cappello, A. and Toni, A., (2003), "Comparative in vitro study on the long term performance of cemented hip stems: validation of a protocol to discriminate between "good" and "bad" designs", *J. Biomech.*, **36**(11), 1603-1615.

Cuppone, M., Seedhom, B.B., Berry, E., Ostell and A.E., (2004), "The longitudinal Young's modulus of cortical bone in the midshaft of human femur and its correlation with CT scanning data", *Calcified Tissue Int.*, **74**(3), 302-309.

Dickenson, R.P., Hutton, W.C. and Stott, J.R.R., (1981), "The mechanical properties of bone in osteoporosis.", *J. Bone Joint Surg.*, **63-B**(2), 233-238.

Duchemin, L., Bousson, V., Raossanaly, C., Bergot, C., Laredo, J.D., Skalli, W. and Mitton, D., (2008), "Prediction of mechanical properties of cortical bone by quantitative computed tomography", *Med. Eng. Phys.*, **30**(3), 321-328.

Duda, G.N., Heller, M., Albinger, J., Schultz, O., Schneider, E. and Claes, L. (1998), "Influence of muscle forces on femoral strain distribution", *J. Biomech.*, **31**(9), 841-846.

Evans, F.G., (1969), "The mechanical properties of bone", *Artificial Limbs*, **13**, 37-48.

Evans, F.G., (1976), "Mechanical properties and histology of cortical bone from younger and older men", *The Anatomical Record*, **185**(1), 1-11.

Gardner, M.P., Chong, A.C.M., Pollock, A.G. and Wooley, P.H., (2010), "Mechanical evaluation of large-size fourth-generation composite femur and tibia models", *Ann. Biomed. Eng.,* **38**(3), 613-620.

Garelick, G., Kärrholm, J., Rogmark, C., and Hernerts, P., (2009), "*Swedish hip arthroplasty register annual report.* Sweden: Department of orthopaedics", Sahlgrenska University Hospital, Sweden.

Goldstein, S.A., (1987), "The mechanical properties of trabecular bone dependance on anatomic locationand function", *J. Biomech.*, **20**(11-12), 1055-1061.

Grant, J.A., Bishop, N.E., Götzen, N., Specher, C., Honl, M. and Morlock, M. (2007), "Artificial composite bone as a model of human trabecular bone: the implant-bone interface", *J. Biomech.,* **40**(5), 1158-1164.

Heiner, A.D., (2008), "Structural properties of fourth-generation composite femurs and tibias", *J. Biomech.*, **40**(15), 3615-3625.

Helgasson, B., Perilli, E., Schileo, E., Taddei, F., Brynjolfsson, S. and Viceconti, M., (2008), "Mathematical relationships between bone density and material properties: A literature review", *Clin. Biomech.*, **23**(2), 135-146.

Hong, J., H. Cha, Y. Park, S. Lee, G. Khang and Y. Kim, (2007), "Elastic moduli and Poisson's ratios of microscopic human femoral trabeculae", *11th Mediterranean Conference on Medical and Biomedical Engineering and Computing.*, Ljubljana, Springer, Slovenia.

Howard, J.L., Hui, A.J., Bourne, R.B., McCalden, R.W., McDonald, S.J. and Rorabeck, C.H., (2004), "A quantitative analysis of bone support comparing cementless tapered and distal fixation total hip replacement", *J. Arthroplasty.*, **19**(3), 266-273.

Jiang, Y., Zhao, J., Augat, P., Ouyang, X., Lu, Y., Majumbar, S. and Genant, H.K., (1998), "Trabecular bone mineral and calculated structure of human bone specimens scanned by peripheral quantitative computed tomography: Relation to biomechanical properties", *J. Bone Miner. Res.*, **13**(11), 1783-1790.

Jirousek, O., (2012), "Nanoindentation of human trabecular bone-tissue mechanical properties compared to standard engineering test methods", Chapter 11, InTech, Rijeka, Croatia.

Joshi, M.G., Advani, S.G., Miller, F. and Santare, M.H., (2000), "Analysis of a femoral hip prosthesis designed to reduce stress shielding", *J. Biomech.*, **33**(12), 1655-1662.

Kaneko, T.S., Pejcic, M.R., Tehranzadeh, J., Keyak, J.H., (2003), "Relationships between material properties and CT scan data of cortical bone with and without metastatic lesions", *Med. Eng. Phys.*, **25**(6), 445-454.

Kassi, J.P., Heller, M.O., Stoeckle, U., Perka, C.and Duda, G.N., (2005), "Stair climbing is more critical than walking in pre-clinical assessment of primary stability in cementless THA in vitro", *J. Biomech.*, **38**(5), 1143-1154.

Keaveny, T.M., Morgan, E.F. and Yeh, O.C., (2004), "Bone mechanics", *Standard Handbook of Biomedical Engineering and Design - Chapter 8*, McGraw-Hill Companies, New York, USA.

Keller, T.S., (1994), "Predicting the compressive mechanical behavior of bone", *J. Biomech.*, **27**(9), 1159-1168.

Keller, T.S., Mao, Z. and Spengler, D.M., (1990), "Young's modulus, bending strength, and tissue physical properties of human compact bone", *J. Orthopaed. Res.*, **8**(4), 592-603.

Kulkarni, M.S. and Sathe, S.R., (2008), "Experimental determination of material properties of cortical cadaveric femur bone", *Trends Biomater. Artif. Organs*, 9-15.

Li, B. and Aspden, R., (1997), "Composition and mechanical properties of cancellous bone from the femoral head of patients with osteoporosis or osteoarthritis", *J. Bone Miner. Res.*, **12**(4), 641-651.

Lotz, J.C., Gerhart, T.N. and Hayes, W.C. (1991), "Mechanical properties of metaphyseal bone in the proximal femur", *J. Biomech.*, **24**(5), 317-329.

Majumbar, S., Kothari, M., Augat, P., Newitt, D.C., Link T.M., Lin, J.C., Lang, T., Lu, Y. and Genant, H.K., (1998), "High-resolution magnetic resonance imaging: three-dimensional trabecular bone architecture and biomechanical properties", *Bone*, **22**(5), 445-454.

McCalden, R.W., McGeough, J.A., Barker, M.B. and Court-Brown, C.M., (1993), "Age-related changes in the tensile properties of cortical bone", *J. Bone Joint Surg.*, **75**(8), 1193-1205.

McKellop, H., Ebramzadeh, E. , Niederer, P.G. and Sarmiento, A., (2005), "Comparison of the stability of press-fit hip prosthesis femoral stems using a synthetic model femur", *J. Orthopaed. Res.*, **9**(2), 297-305.

Mjöberg, B., (1991), "Fixation and loosening of hip prostheses. A review", *Acta. Orthop. Scand.*, **62**(2), 500-508.

Morgan, E.F., Yeh, O.C., Chang, W.C. and Keaveny, T.M., (2001a), "Nonlinear behavior of trabecular bone at small strains", *J. Biomech. Eng.*, **123**(1), 1-9.

Morgan, E.F. and Keaveny, T.M., (2001b), "Dependence of yield strain of human trabecular bone on anatomic site", *J. Biomech.*, **34**(5), 569-577.

Morlock, M., Schneider, E., Blhum, A., Vollmer, M., Bergmann, G., Müller, V. and Honl, M., (2001), "Duration and frequency of everyday activities in total hip patients", *J. Biomech.*, **34**(7), 873-881.

Nazarian, A., Muller, J., Zurakowski, D., Müller and R. Snyder, B.D., (2007), "Densitometric, morphometric, and mechanical distributions in the human proximal femur", *J. Biomech.*, **40**(11), 2573-2579.

Nyman, J.S., Roy, A., Shen, X., Acuna, R.L., Tyler, J.H. and Wang, X., (2006), "The influence of water removal on the strength and toughness of cortical bone", *J. Biomech.*, **39**(5), 931-938.

Ö hman, C., Baleani, M., Perilli, E., Dall'Ara, E., Tassani, S., Baruffaldi F. and Viceconti, M., (2007), "Mechanical testing of cancellous bone from the femoral head: Experimental errors due to off-axis measurements", *J. Biomech.*, **40**(11), 2426-2433.

Ostbyhaug, P.O., Klaksvik, J., Romundstad, P. and Aamodt, A., (2010), "Primary stability of custom and anatomical uncemented femoral stems: a method for three-dimensional in vitro measurement of implant stability", *Clin. Biomech.*, **25**(4), 318-324.

Pancanti, A., Bernakiewicz, M. and Viceconti, M., (2003), "The primary stability of a cementless stem varies between subjects as much as between activities", *J. Biomech.*, **36**(6), 777-785

Papini, M., Zdero, R., Schemitsch, E.H. and Zalzal, P., (2007), "The biomechanics of human femurs in axial and torsional loading: Comparison of finite element analysis, human cadaveric femurs, and synthetic femurs", *J. Biomech. Eng.*, **129**(1), 12-19.

Park, Y., Choi, D.O., Hwang, D.S. and Yoon, Y.S., (2008), "Primary stability of cementless stem in THA improved with reduced interfacial gap", *J. Biomech. Eng.*, **130**(2), 1-7.

Park, Y., Choi, D.O., Hwang, D.S. and Yoon, Y.S. (2009), "Statistical analysis of interfacial gap in a cementless stem FE model", *J. Biomech. Eng.*, **131**(2), 1-8.

Peng, L., Bai, J., Zeng, X. and Zhou, Y., (2006), "Comparison of isotropic and orthotropic material property assignments on femoral finite element models under two loading conditions", *Med. Eng. Phys.*, **28**(3), 227-233.

Pilliar, R.M., Lee, J.M. and Maniapoulos, C., (1986), "Observation of the effect of movement on bone ingrowth into porous-surfaced implants", *Clin. Orthop. Relat. Res.*, **208**, 108-113.

Pivec, R., Johnson, A.J., Mears, S.C. and Mont M.A., (2012), "Hip arthroplasty", *Lancet*, **380**(9855), 1768-1777.

Reilly, D.T. and Burnstein, A.H., (1974), "The mechanical properties of cortical bone", *J. Bone Joint Surg.*, **56**(5), 1001-1022.

Reimeringer, M., Gardan, N. Gardan, Y. and Ugur, H., (2008), "CADFORSIM: Rules to improve the mesh quality", *Proceedings of the 7th International Symposium on Tools and Methods for Concurrent Engineering (TMCE2008),* Izmir, Turkey.

Reimeringer, M., Nuño, N., Desmarais-Trépanier, C., Lavigne, M. and Vendittoli, P.A., (2013a), "The influence of uncemented femoral stem length and design on its primary stability: a finite element analysis", *Comput. Methods Biomech. Biomed. Eng.*, **16**(11), 1221-1231.

Reimeringer M., Nuño, N., (2013b),"Evaluation of the micromotion as a function of the area where press-fit is applied for a cementless hip implant", *Bone Joint J.*, **95-B** no. SUPP 34, 158.

Rohlmann, A., Zilch, H., Bergmann, G. and Kölbel R., (1980), "Material properties of femoral cancellous bone in axial loading Part 1: Time independant properties", *Arch. Orthop. Trauma Surg.,* **97**(4), 95-102.

Sawbones (2013), http://www.sawbones.com/Content/AboutUs_SawbonesCatalog

Schoenfeld, C.M., Lautenschlager, E.P. and Meyer, P.R., (1974), "Mechanical properties of human cancellous bone in the femoral head", *Med. Biol. Eng.*, **12**(3), 313-317.

Sitzer, A., Wendlandt, R., Barkhausen, J., Kovacs, A., Weyers, I. and Schultz, A.P., (2012), "Determination of material properties related to quantitative CT in human femoral bone for patient specific finite element analysis - A comparison of material laws", *Webmed Central Orthopaedics*, **3**(7), 1-12.

Speirs, A.D., Heller, M.O., Duda, G.N. and Taylor, W.R., (2007a), "Physiologically based boundary conditions in finite element modelling", *J. Biomech.*, **40**(10), 2318-2323.

Speirs, A.D., Heller, M.O., Taylor, W.R., Duda, G.N. and Perka, C., (2007b), "Influence of changes in stem positioning on femoral loading after THA using a short-stemmed hip implant", *Clin. Biomech.*, **22**(4), 431-439.

Thielen, T., Maas, S., Zuerbes, A., Waldmann, D., Anagnostakos, K.and Kelm, J., (2009), "Mechanical behaviour of standardized, endoskelton-including hip spacers implanted into composite femurs", *Int. J. Med. Sci.*, **6**(5), 280-286.

Tomsen, M.N., Breusch, S.J., Aldinger P.R., Götz, W., Lahmer, A., Honl, M., Birke, A. and Nägel, H., (2002), "Robotically-milled bone cavities - A comparison with hand broaching in different types of cementless hip stems", *Acta Orthop. Scand.*, **73**(4), 379-385.

Turner, C.H., Rho, J., Takano, Y., Tsui, T. and Pharr, G.M., (1999), "The elastic properties of trabecular and cortical bone tissues are similar: results from two microscopic measurement techniques", *J. Biomech.*, **32**(4), 437-441.

Viceconti, M., Monti, L., Muccini, R., Bernakiewicz, M. and Toni, A., (2001), "Even a thin layer of soft tissue may compromise the primary stability of cementless hip stems", *Clin. Biomech.*, **16**(9), 765-775.

Viceconti, M., Casali, M., Massari, M., Cristofolini, L., Bassini, S. and Toni, A., (1996), "The standardized femur program proposal for a reference geometry to be used for the creation of finite element models of the femur", *J. Biomech.*, **29**(9), 1241.

Viceconti, M., Muccini, R., Bernakiewicz, M., Baleani, M. and Cristofolini, L., (2000), "Large-sliding contact elements accurately predicts levels of bone-implant micromotion relevant to osteointegration", *J. Biomech.*, **33**(12), 1611-1618.

Wall, J.C., Chatterji, S.K. and Jeffery, J.W., (1979), "Age-related changes in the density and tensile strength of human femoral cortical bone", *Calcified Tissue Int.*, **27**(2), 105-108.

Wirtz, D.C., Schiffers, N., Pandorf, T., Radermacher, K., Weichert, D. and Forst, R., (2000), "Critical evaluation of known bone material properties to realize anisotropic FE-simulation of the proximal femur", *J. Biomech.*, **33**(10), 1325-1330.

Wong, A.S., New, A.M.R., Isaacs, G. and Taylor, M., (2005), "Effect of bone material properties on the initial stability of a cementless hip stem: a finite element study", *Proc. Inst. Mech. Eng. H.*, **219**(4), 265-275.

Wu, L.D., Hahne, H.J. and Hassenpflug J., (2004), "The dimensional accuracy of preparation of femoral cavity in cementless total hip arthroplasty", *J. Zheijiang Univ. Sci.*, **5**(10), 1270-1278.

MC

Appendix

Appendix A – Material properties of cancellous bone realised on sample size comprised between 5mm and 40mm

Authors	Zones	Tests	Specimens	Young modulus (MPa)
(Evans 1969)	Head	Compression	69 rectangular (R) 15 cubic (C)	R=275 ; C=450
	Lateral condyle			R=275 ; C=195
	Medial condyle			R=205 ; C=175
	Neck			C=380
	Great trochanter			C=172
(Schoenfeld *et al.* 1974)	Head	Compression	30	344
(Brown *et al.* 1978)	Head	Compression	300	SI^1 = 334.4
				AP^2 = 223.8
				ML^3 = 250.9
(Rohlmann *et al.* 1980)	Head	Compression	42	308
	Condyles		42	497
(Brown *et al.* 1980)	Proximal femur	Compression	800	SI^1 = 338.6
				AP^2 = 259.5
				ML^3 = 196.7
(Li *et al.* 1997)	Head	Compression	7 normal	310
			17 osteoporosis	247
			16 osteoarthritis	356
(Majumbar *et al.* 1998)	Proximal femur	Compression	47	SI^1 = 130.2
				AP^2 = 51.2
				ML^3 = 56.7
				Mean = 77.8
	Distal femur		47	SI^1 = 118.8
				AP^2 = 40.2
				ML^3 = 59.6
				Mean = 73.5
(Jiang *et al.* 1998)	Proximal femur	Compression	11	141
	Distal femur		14	89
(Augat *et al.* 1998)	Proximal femur	Compression	29	SI^1 = 137
				AP^2 = 54
				ML^3 = 68
	Distal femur		33	SI^1 = 105
				AP^2 = 54
				ML^3 = 31

(Morgan *et al.* 2001a)	Great trochanter	Compression	10	564
		Tension	13	522
	Neck	Tension	13	2348
	Great trochanter	Compression	10	601
		Tension	13	569
	Neck	Tension	13	2566
(Morgan *et al.* 2001b)	Neck	Compression	56	622
		Tension		597
	Great trochanter	Compression	33	3230
		Tension		2700
(Birnbaum *et al.* 2002)	Head	Compression	36 proximal	146 - 320
			36 medial	73.7 – 320
			36 distal	50.9 – 280
(Brown *et al.* 2002)	Head	Compression	11 normal superior	$AP^2 = 247$
			11 normal inferior	$AP^2 = 51$
			21 osteoarthritis superior	$AP^2 = 226$
			21 osteoarthritis inferior	$AP^2 = 58$
(Hong *et al.* 2007)	Head	Compression	21	$SI^1 = 3747$
				$AP^2 = 2570$
				$ML^3 = 2540$
(Nazarian *et al.* 2007)	Proximal femur	Compression	14 heads 28 necks 7 trochanteric regions (E_{S1}, E_{S2}, E_{S3}, E_{S4}, E_{S5}, E_{S6})	$E_{S1} = 187$
				$E_{S2} = 329$
				$E_{S3} = 263$
				$E_{S4} = 175$
				$E_{S5} = 137$
				$E_{S6} = 166$
				$E_{S7} = 170$
(Ö hman *et al.* 2007)	Head	Compression	10	Aligned with MTD8 → 2730
				20° misalignement with MTD8 → 1590
(Burgers *et al.* 2008)	Condyles	Compression	28	$SM^4 = 131$
				$SL^5 = 208$
				$IM^6 = 390$
				$IL^7 = 664$

[1]superior-inferior [2]anterior-posterior [3]medial-lateral [4]superior-medial [5]superior-lateral [6]inferior-medial [7]inferior-lateral [8]Main trabecular direction

Michael Reimeringer and Natalia Nuño

Appendix B: Material properties of cortical bone realised on sample size comprised between 5mm and 40mm

Authors	Zones	Tests	Specimens	Young modulus (GPa)
(Reilly *et al.* 1974)		Tension		Longitudinal = 17
				Transverse = 11.5
(Evans 1976)	Midschaft	Tension	35 younger	14.9
			35 older	13.6
(Burnstein *et al.* 1976)	Diaphysis	Tension	178	[15.7 – 17.7]
		Compression	95	[14.4 – 18.7]
(Dickenson *et al.* 1981)	Midshaft	Tension	30 osteoporotic	11.554 [3.975-18.34]
			29 normal	15.686 [12.694-19.427]
(Carter *et al.* 1981)	Mid diaphysis	Tension	10	17.5
(Keller *et al.* 1990)	Midschaft	3-point bending	68 proximal	[12.2-15.7]
			87 distal	[9.82-13.1]
(Lotz *et al.* 1991)	Diaphysis	3-point bending	36	Longitudinal = 12.5 Transverse = 5.99
	Proximal femur		123	Longitudinal = 9.65 Transverse = 5.47
(McCalden *et al.* 1993)	Mid diaphysis	Tension	235	[9-22]
(Keller 1994)		Compression	297	[16.2-17]
(Courtney *et al.* 1996)	Diaphysis	Tension	28 elderly	Initial = 14.78
				Reloaded = 9.87
			28 young	Initial = 15.69
				Reloaded = 10.32
(Turner *et al.* 1999)	Midschaft	Nanoindentation	1	Transversal = 16.58
(Kaneko *et al.* 2003)	Diaphysis	Tension	17	22.7 [19.3 - 26.3]
		Compression	16	23 [20.4 - 26.4]
(Keaveny *et al.* 2004)				Longitudinal = 17.9 Transverse = 10.1 Shear = 3.3
(Cuppone *et al.* 2004)	Midschaft	3-point bending	180	18.6
(Nyman *et al.* 2006)	Mid diaphysis	3-point bending	36	[9.9 – 15.5]
(Kulkarni *et al.* 2008)		Compression		11.737
		Tension		8.755
		Torsion		7.896
(Duchemin *et al.* 2008)	Mid diaphysis	Compression	46	11.8
		Tension	46	14.3
(Sitzer *et al.* 2012)	Mid diaphysis	Compression	5	Longitudinal [17.13 - 19.56]
		Compression	5	Transverse [6.6 - 12.02]
		3-point bending	5	[16.17 - 19.14]